HHS Public Access

Author manuscript

Nature. Author manuscript; available in PMC 2021 December 02.

Published in final edited form as:

Nature. 2020 December ; 588(7837): 254–260. doi:10.1038/s41586-020-2919-z.

Catalytic Asymmetric Addition of an Amine N-H Bond Across Internal Alkenes

Yumeng Xi, **Senjie Ma**, **John F. Hartwig**

Department of Chemistry, University of California, Berkeley, and Division of Chemical Sciences, Lawrence Berkeley National Laboratory, Berkeley, CA 94720, USA.

Hydroamination of alkenes, the addition of the N-H bond of an amine across an alkene, is a fundamental, yet challenging organic transformation that creates an alkylamine from two abundant chemical feedstocks, alkenes and amines, with full atom economy.[1–3] The reaction is particularly important because amines, especially chiral amines, are prevalent substructures in a wide range of natural products and drugs. Although extensive efforts have been dedicated to developing catalysts for hydroamination, the vast majority of the alkenes that undergo intermolecular hydroamination have been limited to conjugated, strained, or terminal alkenes;[2–4] only a few examples occur by the direct addition of the N-H bond of amines across unactivated internal alkenes,[5–7] including recent photocatalytic hydroamination,[8,9] and enantioselective intermolecular additions to such alkenes are not known. In fact, current examples of direct, enantioselective intermolecular hydroamination of any type of unactivated alkene lacking a directing group occur with only moderate enantioselectivity.[10–13] Here we report a cationic iridium system that catalyzes intermolecular hydroamination of a range of unactivated, internal alkenes, including those in both acyclic and cyclic alkenes, to afford chiral amines with high enantioselectivity. The catalyst contains a new ligand and triflimide counteranion, and the reaction design includes 2-amino-6-methylpyridine as the amine to enhance the rates of multiple steps within the catalytic cycle, while serving as an ammonia surrogate. These design principles point the way to the additions of N-H bonds of other reagents, as well as O-H and C-H bonds, across unactivated internal alkenes to streamline the synthesis of functional molecules from basic feedstocks.

Chiral amines are essential structural motifs in numerous active pharmaceutical ingredients and in many agrochemicals, and materials. They also serve as chiral catalysts, resolving reagents, and chiral auxiliaries.[14] Thus, efficient methods to prepare chiral amines have been long sought. Traditional approaches[15] include chemical[16,17] and enzymatic[18]

Correspondence and requests for materials should be addressed to J.F.H. (jhartwig@berkeley.edu).

Author Contributions

Y.X. and J.F.H. conceived the project. Y.X. discovered the reaction and performed experiments and DFT calculations. S.M. performed experiments for revision. Y.X. and J.F.H. wrote the manuscript.

Data Availability

The data that support the findings of this study are available within the article and its Supplementary Information.

Competing Interests

The authors declare no competing interests.

reductive amination, hydrogenation,[19] nucleophilic addition to imines,[20] and nucleophilic substitution.[21,22] However, these methods require starting materials containing reactive functionality that is often derived from feedstock alkenes. Thus, hydroamination of alkenes is the most direct method to construct chiral amines from a functional group that is present in basic feedstocks and is typically unprotected. Asymmetric additions to conjugated alkenes, such as dienes[23–26] and vinylarenes,[27,28] have been reported, but the scope of the direct addition of N-H bonds to more common and less reactive, unconjugated alkenes is severely limited, and the enantioselectivities of asymmetric processes are far below those that would enable applications for the synthesis of chiral amines. Formal hydroaminations provide an alternative approach to this problem, but the use of silanes with electrophilic aminating reagents[29] and even metal reductants,[30] instead of amines, undermines the atom-economy of the hydroamination reaction. Direct N-H additions of unactivated internal alkenes that occur with high enantioselectivity are unknown.

Significant challenges confront the development of catalytic hydroaminations of unactivated alkenes that bear more than one substituent (Fig. 1A). Both experiments and theoretical studies have shown that the thermodynamic driving force is weak, and the kinetic barrier to combining two nucleophiles is high.[1,31] Moreover, catalysts for hydroamination often catalyze undesirable, competing alkene isomerization, and isomerization is typically faster than addition of the N-H bond during many metal-catalyzed hydroaminations (Fig. 1B). Such relative rates lead to a mixture of isomeric products.[32,33] Many catalysts for alkene hydroamination also promote formation of oxidative amination products by β-hydrogen elimination of β-aminoalkylmetal intermediates.[34,35] These isomerization and oxidative side reactions must be suppressed to achieve hydroamination of unactivated internal alkenes. Finally, because hydroamination is usually close to ergoneutral, isomerization and racemization of the products during the reaction can erode regioselectivity and enantioselectivity.[36]

To address these challenges, we modified a prior neutral iridium complex containing a bisphosphine ligand, which had catalyzed the formation of hydroamination and oxidative amination products from the reaction of terminal alkenes with amides and indoles.[34,37–40] We had shown that the reaction occurred by a mechanism comprising oxidative addition of N-H bonds, migratory insertion of alkenes, and reductive elimination of C-H bonds.[34] We envisioned that switching the iridium catalyst from neutral to cationic would lead to the formation of cationic iridium intermediates that would undergo migratory insertion of the alkene more rapidly,[41] a step that was shown to be rate-limiting in the reaction of terminal alkenes with the neutral catalyst (Fig. 1C).[34] If binding and insertion of the alkene were sufficiently enhanced, then the reaction scope might include internal alkenes. In addition, we envisioned that coordinating groups adjacent to the amine (e.g. 2-aminopyridine derivatives) could facilitate and make more thermodynamically favorable the initial N-H oxidative addition, and such enhancements of this step could be important because the rate of oxidative addition of electron-deficient metal complexes is generally slower than that of electron-rich ones.[42] If properly placed, the coordinating groups of the amine also could form a rigid 6-membered iridacycle upon insertion of the alkene; this geometry could suppress β-hydrogen elimination to form enamines. Such a combination of 2-aminopyridine and a cationic iridium catalyst was evaluated by Shibata for the hydroamination of terminal

vinylarenes, but only briefly for the hydroamination of unactivated α-alkenes.[12] Low enantioselectivities (≤11% ee) were observed, and the reactions of unstrained internal alkenes were not examined. We reasoned that a substituent nearby the binding group of the amine could modulate the strength of the coordination of the pyridine, leading to potential enhancement of the activity of the iridium catalyst, due to weakened coordination (Fig. 1C). Finally, the pyridyl group of the product could be cleaved by known methods to reveal the corresponding primary amine.[43]

Fig. 2 summarizes our studies to develop a cationic iridium catalyst and an ammonia surrogate for the asymmetric hydroamination of unactivated internal alkenes. These experiments revealed the role of reaction components of the system on reaction yield, level of alkene isomerization, and enantioselectivity. To identify a suitable ammonia surrogate for this reaction, we surveyed a series of heteroaromatic amines that possess varying structural properties. The hydroamination products from these reactions consisted of three isomers (denoted **A**, **B** and **C)** that likely resulted from competing alkene isomerization and hydroamination. A larger amount of **A** reflects a faster rate for direct addition of the amine to the starting alkene than alkene isomerization prior to addition.

As shown in Fig. 2A, hydroamination of *cis*-4-octene in the presence of $[Ir(coe)_2Cl]_2$, (*S*)-DTBM-SEGPHOS [(*S*)-(+)-5,5'-Bis[di(3,5-di-tert-butyl-4-methoxyphenyl)phosphino]-4,4'-bi-1,3-benzodioxole], and NaBARF [sodium tetrakis[3,5-bis(trifluoromethyl)phenyl]borate] occurred only when 6-substituted 2-aminopyridine derivatives were used as the amine source. The hydroamination of 2-amino-6-methylpyridine formed amines **A**, **B** and **C** in a combined 73% yield with **A** constituting 28% of the amine products (defined as **A**/(**A**+**B**+**C**)). The reaction of 2-amino-6-trifluoromethylpyridine afforded only 5% of isomer **A**. Other amines tested, including the parent 2-aminopyridine, did not undergo this hydroamination. These results suggest that the substituent in the 6-position of the pyridine ring is essential to promote the hydroamination.

To suppress competing alkene isomerization and improve the reaction yield, we examined catalysts containing a series of bisphosphine ligands and counteranions for hydroamination with 2-amino-6-methylpyridine as the amine. Studies of the electronic and steric properties of ligands indicated that the ligands that are less electron-rich (Fig. 2B, entry 2) and more sterically encumbered (Fig. 2B, entries 3–5) than (*S*)-DTBM-SEGPHOS form catalysts that are more reactive and selective for the direct addition to form amine **1**. The observed higher reactivity of catalysts generated from more electron-poor ligands likely results from a greater rate of migratory insertion of the alkene (*vide infra*) into the Ir-N bond of complexes containing **L2**-**L5** lacking the methoxy group than into the Ir-N bond of the complex ligated by (*S*)-DTBM-SEGPHOS possessing the *p*-OMe group.[44] The higher selectivity from the more hindered ligands could result from a greater sensitivity of the rate of insertion of the alkene into the metal-amido bond (Fig. 1C, structure **II**) to steric effects than the rate of insertion into the metal-hydride bond, which likely leads to alkene isomerization.[45,46] Studies with various counterions revealed that reactions with triflimide as the counterion of the catalyst, instead of other potential counterions, occurred with the highest selectivity at high conversion (Fig. 2B, entries 6–9). The origin of the effects of the counterions is difficult to ascertain, but an effect is clear. Control experiments showed that the reaction catalyzed

by a neutral iridium complex under otherwise identical conditions (Fig. 2B, entry 10) resulted in the exclusive formation of oxidative amination products. By combining the chiral ligand that led to the highest selectivity with the triflimide anion in the form of [((*R*)-TMS-SYNPHOS)Ir(COD)]NTf_2, the model hydroamination reaction formed the 4-aminooctane (**1**) in high yield; this reaction also occurred with remarkably high enantioselectivity (Fig. 2B, entry 11). Thus, the substituent on the amine, the new phosphine ligand, and the use of triflimide counterion all led to the high activity, chemoselectivity, and enantioselectivity of the reaction.

With this catalyst and reagent, we examined the scope of alkenes that underwent hydroamination (Fig. 3). Both symmetrical internal alkenes and unsymmetrical internal alkenes underwent hydroamination with 2-amino-6-methylpyridine. The reactions all proceeded in greater than 90% ee. Hydroamination of symmetrical alkenes afforded products containing linear alkyl groups (**1**), aryl-substituted alkyl groups (**2**), and branched alkyl groups (**3**), silyloxy groups (**4**), alkoxy groups (**5**), and alkoxycarbonyl groups (**6**) in good to high yields. Reactions of unsymmetrical internal alkenes bearing polar functional groups at the homoallylic position occurred with synthetically useful regioselectivity (2:1 to 10:1). These functional groups include phthalimidyl groups (**7**,**8**), sulfonamido groups (**9**), silyloxy groups (**10**), bis(ethoxycarbonyl)methyl groups (**11**), and (hetero)aryloxy groups (**12**-**14**). These groups presumably influence the regioselectivity by inductive effects that are similar to those observed for other classes of functionalization of unsymmetrical internal alkenes.[47–49]

The reactivity of the system for *Z*-alkenes enabled the hydroamination of cyclic alkenes to occur, and these reactions also occurred with high enantioselectivity. The combination of $[Ir(coe)_2Cl]_2$, (*S*)-DTBM-SEGPHOS, and NaBARF was used as the catalyst because it was more reactive than [((*R*)-TMS-SYNPHOS)Ir(COD)]NTf_2 for the hydroaminations of cyclic alkenes. The cyclic hydrocarbons cyclopentene, cyclohexene, cycloheptene, and cyclooctene all underwent hydroamination in high yields (**15**-**18**). The hydroamination of a series of substituted cyclopentenes formed chiral amine products with high enantioselectivity (**19**-**23**, 90–92% ee). The reaction to form the 1,3-substituted cyclopentane **23** from the 4-methoxycarbonyl-substituted cyclopentene occurred with high diastereoselectivity for the *trans* product. In addition, cyclohexenes derivatives with 3,3-substituents underwent hydroamination to afford two products with regioselectivity of approximately 1:3 (**24**/**24'**,**25**/**25'**). Although the major isomer is achiral, the chiral minor isomer was formed with good to high enantioselectivity. We observed in some cases that the hydroaminations of substituted cycloalkenes with rings larger than five occurred to high conversion, but were complicated by competing alkene isomerization, which led to mixtures of isomers that were difficult to separate.

The pyridyl group of the hydroamination products (**1**, **9**) was cleaved by a short sequence that consisted of protonation, hydrogenation, and borohydride reduction. The corresponding primary amines (**26**, **27**) formed in 71–85% yield with little or no erosion in enantiomeric excess (see Supplementary Information sections VI and X). By the same sequence, hydroamination product **6** was converted to the corresponding δ-lactam (**28**) in 79% yield.

To understand how the combination of a cationic iridium catalyst and 2-amino-6-methylpyridine enabled the hydroamination of unactivated internal alkenes, we conducted studies to investigate the reaction mechanism. The reaction of a substituted cyclopentene with *N, N*-dideuterio-2-amino-6-methylpyridine showed that the addition occurred in a *syn* fashion. This stereochemistry is consistent with a mechanism that involves migratory insertion of an alkene, rather than nucleophilic attack on a metal-bound alkene complex (Fig. 4A). Kinetic experiments showed that the reaction is first order in [iridium catalyst], positive order in [*cis*-4-octene], and inverse order in [2-amino-6-methylpyridine] (Fig. 4B). These data suggest that a molecule of 2-amino-6-methylpyridine dissociates reversibly from iridium in the catalyst resting-state prior to rate-limiting insertion of the alkene, presumably into the metal-amido bond.[41] To elucidate why the methyl group of 2-amino-6-methylpyridine is essential in this reaction, we conducted the hydroamination of *cis*-4-octene with equimolar amounts of 2-amino-6-methylpyridine and 2-aminopyridine. While the reaction of 2-amino-6-methylpyridine alone afforded the hydroamination product in high yield, the reaction that contained both 2-amino-6-methylpyridine and 2-aminopyridine provided neither hydroamination product (Fig. 4C). This result implies that stronger binding of the 2-aminopyridine than of 2-amino-6-methylpyridine inhibits the catalyst. It also implies that the methyl group of 2-amino-6-methylpyridine weakens the binding to the iridium center, thereby allowing for alkene binding and insertion.

To investigate the origin of the high levels of enantioselectivity in the hydroamination, we conducted calculations on the alkene migratory insertion with density functional theory (DFT). Based on the kinetic experiments, this step is likely the rate-limiting and enantio-determining step of the catalytic cycle. We calculated 12 possible isomeric transition states of migratory insertion that would lead to either enantiomer of the products with *cis*-2-butene as the model alkene. The structures of the lowest-energy transition states that lead to the major and minor enantiomers are illustrated in Fig. 4D. The two transition states of many metal-catalyzed enantioselective hydrofunctionalization reactions of alkenes to form two enantiomers differ principally by the face of the alkene to which the metal is bound. In the current system, the orientation of ancillary ligands around the metal, in addition to the face of the alkene, differs greatly in the two transition states. The geometry of **TS-1a**, the transition state leading to the major enantiomer, contains meridionally oriented hydride, pyridine, and amido ligands with the hydride trans to the amido group. In contrast, these three ligands in **TS-2a**, which is the lowest-energy transition state leading to the minor enantiomer, are arranged with the hydride trans to the pyridine donor. The geometry analogous to **TS-1a** that would form the opposite enantiomer by orienting the methyl groups away from the pyridine ligand (**TS-2c** and **TS-2d**, Scheme S4) is higher in energy than **TS-2a. TS-1a** is likely the lowest energy transition state for several reasons. First, the Ir-N_{am} bond to the amido group, which is trans to a hydride in **TS-1a**, is elongated (2.32 Å), thereby leading to higher reactivity toward insertion. Second, the alkene is perpendicular to the P-Ir-P plane in **TS-1a**, whereas the alkene is almost co-planar with the P-Ir-P plane in **TS-2a**. These orientations place the substituents on the alkene in **TS-1a** further from the phosphine ligand than those on the alkene in **TS-2a**, leading to less steric hindrance in **TS-1a** than in **TS-2a**. This analysis suggests that electronic and steric effects together impart high enantioselectivity in the hydroamination.

Our work demonstrates the direct N-H addition of amines to unactivated internal alkenes can occur with high enantioselectivity under thermal conditions, without the need for strategies involving formal hydroamination. Despite the typically high barriers and weak thermodynamic driving force for hydroamination, the cationic bisphosphine-ligated iridium as catalyst and 2-amino-6-methylpyridine as the amine led to enhancements of the rates of multiple steps within the catalytic cycle and suppression of alkene isomerization and oxidative amination, enabling the hydroamination of unactivated internal alkenes in high yield and with high enantioselectivity. The hydroamination products can be converted to the corresponding primary amines readily with preservation of the high enantiomeric excess of the hydroamination products. These design principles should provide a starting point to address the long-standing challenge of applying hydroamination of unactivated internal alkenes to the synthesis of chiral amines and inspire advances in other asymmetric hydrofunctionalizations of internal alkenes.

Supplementary Material

Refer to Web version on PubMed Central for supplementary material.

Acknowledgements

The enantioselective aspects of the work were supported by the National Institutes of Health under grant R35GM130387 and the catalyst development was supported by the Director, Office of Science, of the U.S. Department of Energy under contract No. DE-AC02–05CH11231. Calculations were performed at the Molecular Graphics and Computation Facility at UC Berkeley funded by the NIH (S10OD023532). We gratefully acknowledge Takasago for gifts of (*S*)-DTBM-SEGPHOS, and Dr. Hasan Celik for assistance with NMR experiments. Instruments in the CoC-NMR are supported in part by NIH S10OD024998. We thank Prof. Bob Bergman, Prof. Bo Su, and Trevor Butcher for helpful discussions. Y.X. thanks Bristol-Myers Squibb for a graduate fellowship, Shayun Pedram for supply of NaBARF, and Dr. Dave Small for assistance with DFT calculations.

References

1. Müller TE & Beller M. Metal-Initiated Amination of Alkenes and Alkynes. Chem. Rev 98, 675–704 (1998). [PubMed: 11848912]
2. Müller TE, Hultzsch KC, Yus M, Foubelo F. & Tada M. Hydroamination: Direct Addition of Amines to Alkenes and Alkynes. Chem. Rev 108, 3795–3892 (2008). [PubMed: 18729420]
3. Huang L, Arndt M, Gooßen K, Heydt H. & Gooßen LJ Late Transition Metal-Catalyzed Hydroamination and Hydroamidation. Chem. Rev 115, 2596–2697 (2015). [PubMed: 25721762]
4. Reznichenko AL & Hultzsch KC in Hydroamination of Alkenes. In Organic Reactions 1–554 (2015).
5. Gurak JA, Yang KS, Liu Z. & Engle KM Directed, Regiocontrolled Hydroamination of Unactivated Alkenes via Protodepalladation. J. Am. Chem. Soc 138, 5805–5808 (2016). [PubMed: 27093112]
6. Karshtedt D, Bell AT & Tilley TD Platinum-Based Catalysts for the Hydroamination of Olefins with Sulfonamides and Weakly Basic Anilines. J. Am. Chem. Soc 127, 12640–12646 (2005). [PubMed: 16144412]
7. Zhang J, Yang C-G & He C. Gold(I)-Catalyzed Intra- and Intermolecular Hydroamination of Unactivated Olefins. J. Am. Chem. Soc 128, 1798–1799 (2006). [PubMed: 16464072]
8. Musacchio AJ et al. Catalytic intermolecular hydroaminations of unactivated olefins with secondary alkyl amines. Science 355, 727–730 (2017). [PubMed: 28209894]
9. Nguyen TM, Manohar N. & Nicewicz DA anti-Markovnikov Hydroamination of Alkenes Catalyzed by a Two-Component Organic Photoredox System: Direct Access to Phenethylamine Derivatives. Angew. Chem. Int. Ed 53, 6198–6201 (2014).

10. Zhang Z, Lee SD & Widenhoefer RA Intermolecular Hydroamination of Ethylene and 1-Alkenes with Cyclic Ureas Catalyzed by Achiral and Chiral Gold(I) Complexes. J. Am. Chem. Soc 131, 5372–5373 (2009). [PubMed: 19326908]
11. Reznichenko AL, Nguyen HN & Hultzsch KC Asymmetric Intermolecular Hydroamination of Unactivated Alkenes with Simple Amines. Angew. Chem. Int. Ed 49, 8984–8987 (2010).
12. Pan S, Endo K. & Shibata T. Ir(I)-Catalyzed Intermolecular Regio- and Enantioselective Hydroamination of Alkenes with Heteroaromatic Amines. Org. Lett 14, 780–783 (2012). [PubMed: 22256899]
13. Vanable EP et al. Rhodium-Catalyzed Asymmetric Hydroamination of Allyl Amines. J. Am. Chem. Soc 141, 739–742 (2019). [PubMed: 30614700]
14. Nugent TC Chiral Amine Synthesis: Methods, Developments and Applications. (Wiley VCH, 2010).
15. Trowbridge A, Walton SM & Gaunt MJ New Strategies for the Transition-Metal Catalyzed Synthesis of Aliphatic Amines. Chem. Rev 120, 2613–2692 (2020). [PubMed: 32064858]
16. Wang C. & Xiao J. in Stereoselective Formation of Amines (eds Li Wei & Zhang Xumu) 261–282 (Springer Berlin Heidelberg, 2014).
17. Nugent TC & El-Shazly M. Chiral Amine Synthesis – Recent Developments and Trends for Enamide Reduction, Reductive Amination, and Imine Reduction. Adv. Synth. Catal 352, 753–819 (2010).
18. Patil MD, Grogan G, Bommarius A. & Yun H. Oxidoreductase-Catalyzed Synthesis of Chiral Amines. ACS Catal. 8, 10985–11015 (2018).
19. Xie J-H, Zhu S-F & Zhou Q-L Transition Metal-Catalyzed Enantioselective Hydrogenation of Enamines and Imines. Chem. Rev 111, 1713–1760 (2011). [PubMed: 21166392]
20. Ellman JA, Owens TD & Tang TP N-tert-Butanesulfinyl Imines: Versatile Intermediates for the Asymmetric Synthesis of Amines. Acc. Chem. Res 35, 984–995 (2002). [PubMed: 12437323]
21. You S-L, Zhu X-Z, Luo Y-M, Hou X-L & Dai L-X Highly Regio- and Enantioselective Pd-Catalyzed Allylic Alkylation and Amination of Monosubstituted Allylic Acetates with Novel Ferrocene P,N-Ligands. J. Am. Chem. Soc 123, 7471–7472 (2001). [PubMed: 11472198]
22. Ohmura T. & Hartwig JF Regio- and Enantioselective Allylic Amination of Achiral Allylic Esters Catalyzed by an Iridium−Phosphoramidite Complex. J. Am. Chem. Soc 124, 15164–15165 (2002). [PubMed: 12487578]
23. Löber O, Kawatsura M. & Hartwig JF Palladium-Catalyzed Hydroamination of 1,3-Dienes: A Colorimetric Assay and Enantioselective Additions. J. Am. Chem. Soc 123, 4366–4367 (2001). [PubMed: 11457216]
24. Adamson NJ, Hull E. & Malcolmson SJ Enantioselective Intermolecular Addition of Aliphatic Amines to Acyclic Dienes with a Pd–PHOX Catalyst. J. Am. Chem. Soc 139, 7180–7183 (2017). [PubMed: 28453290]
25. Long J, Wang P, Wang W, Li Y. & Yin G. Nickel/Brønsted Acid-Catalyzed Chemo- and Enantioselective Intermolecular Hydroamination of Conjugated Dienes. iScience 22, 369–379 (2019). [PubMed: 31812807]
26. Tran G, Shao W. & Mazet C. Ni-Catalyzed Enantioselective Intermolecular Hydroamination of Branched 1,3-Dienes Using Primary Aliphatic Amines. J. Am. Chem. Soc 141, 14814–14822 (2019). [PubMed: 31436415]
27. Kawatsura M. & Hartwig JF Palladium-Catalyzed Intermolecular Hydroamination of Vinylarenes Using Arylamines. J. Am. Chem. Soc 122, 9546–9547 (2000).
28. Utsunomiya M. & Hartwig JF Intermolecular, Markovnikov Hydroamination of Vinylarenes with Alkylamines. J. Am. Chem. Soc 125, 14286–14287 (2003). [PubMed: 14624571]
29. Yang Y, Shi S-L, Niu D, Liu P. & Buchwald SL Catalytic asymmetric hydroamination of unactivated internal olefins to aliphatic amines. Science 349, 62–66 (2015). [PubMed: 26138973]
30. Gui J. et al. Practical olefin hydroamination with nitroarenes. Science 348, 886–891 (2015). [PubMed: 25999503]
31. Johns AM, Sakai N, Ridder A. & Hartwig JF Direct Measurement of the Thermodynamics of Vinylarene Hydroamination. J. Am. Chem. Soc 128, 9306–9307 (2006). [PubMed: 16848446]

32. Liu Z. & Hartwig JF Mild, Rhodium-Catalyzed Intramolecular Hydroamination of Unactivated Terminal and Internal Alkenes with Primary and Secondary Amines. J. Am. Chem. Soc 130, 1570–1571 (2008). [PubMed: 18183986]
33. Huang J-M, Wong C-M, Xu F-X & Loh T-P $InBr_3$ Catalyzed intermolecular hydroamination of unactivated alkenes. Tetrahedron Letters 48, 3375–3377 (2007).
34. Sevov CS, Zhou J. & Hartwig JF Iridium-Catalyzed Intermolecular Hydroamination of Unactivated Aliphatic Alkenes with Amides and Sulfonamides. J. Am. Chem. Soc 134, 11960–11963 (2012). [PubMed: 22780090]
35. Utsunomiya M, Kuwano R, Kawatsura M. & Hartwig JF Rhodium-Catalyzed Anti-Markovnikov Hydroamination of Vinylarenes. J. Am. Chem. Soc 125, 5608–5609 (2003). [PubMed: 12733880]
36. Pawlas J, Nakao Y, Kawatsura M. & Hartwig JF A General Nickel-Catalyzed Hydroamination of 1,3-Dienes by Alkylamines: Catalyst Selection, Scope, and Mechanism. J. Am. Chem. Soc 124, 3669–3679 (2002). [PubMed: 11929257]
37. Casalnuovo AL, Calabrese JC & Milstein D. Rational design in homogeneous catalysis. Iridium(I)-catalyzed addition of aniline to norbornylene via nitrogen-hydrogen activation. J. Am. Chem. Soc 110, 6738–6744 (1988).
38. Dorta R, Egli P, Zürcher F. & Togni A. The [IrCl(Diphosphine)]2/Fluoride System. Developing Catalytic Asymmetric Olefin Hydroamination. J. Am. Chem. Soc 119, 10857–10858 (1997).
39. Zhou J. & Hartwig JF Intermolecular, Catalytic Asymmetric Hydroamination of Bicyclic Alkenes and Dienes in High Yield and Enantioselectivity. J. Am. Chem. Soc 130, 12220–12221 (2008). [PubMed: 18715004]
40. Sevov CS, Zhou J. & Hartwig JF Iridium-Catalyzed, Intermolecular Hydroamination of Unactivated Alkenes with Indoles. J. Am. Chem. Soc 136, 3200–3207 (2014). [PubMed: 24483848]
41. Hanley PS & Hartwig JF Migratory Insertion of Alkenes into Metal–Oxygen and Metal–Nitrogen Bonds. Angew. Chem. Int. Ed 52, 8510–8525 (2013).
42. Thompson WH & Sears CT Kinetics of oxidative addition to iridium(I) complexes. Inorg. Chem 16, 769–774 (1977).
43. Smout V. et al. Removal of the Pyridine Directing Group from α-Substituted N-(Pyridin-2-yl)piperidines Obtained via Directed Ru-Catalyzed sp3 C–H Functionalization. J. Org. Chem 78, 9803–9814 (2013). [PubMed: 24007399]
44. Hanley PS & Hartwig JF Intermolecular Migratory Insertion of Unactivated Olefins into Palladium–Nitrogen Bonds. Steric and Electronic Effects on the Rate of Migratory Insertion. J. Am. Chem. Soc 133, 15661–15673 (2011). [PubMed: 21815675]
45. Zhang M, Hu L, Lang Y, Cao Y. & Huang G. Mechanism and Origins of Regio- and Enantioselectivities of Iridium-Catalyzed Hydroarylation of Alkenyl Ethers. J. Org. Chem 83, 2937–2947 (2018). [PubMed: 29437389]
46. Xing D, Qi X, Marchant D, Liu P. & Dong G. Branched-Selective Direct α-Alkylation of Cyclic Ketones with Simple Alkenes. Angew. Chem. Int. Ed 58, 4366–4370 (2019).
47. Xi Y, Butcher TW, Zhang J. & Hartwig JF Regioselective, Asymmetric Formal Hydroamination of Unactivated Internal Alkenes. Angew. Chem. Int. Ed 55, 776–780 (2016).
48. Mei T-S, Werner EW, Burckle AJ & Sigman MS Enantioselective Redox-Relay Oxidative Heck Arylations of Acyclic Alkenyl Alcohols using Boronic Acids. J. Am. Chem. Soc 135, 6830–6833 (2013). [PubMed: 23607624]
49. Morandi B, Wickens ZK & Grubbs RH Regioselective Wacker Oxidation of Internal Alkenes: Rapid Access to Functionalized Ketones Facilitated by Cross-Metathesis. Angew. Chem. Int. Ed 52, 9751–9754 (2013).

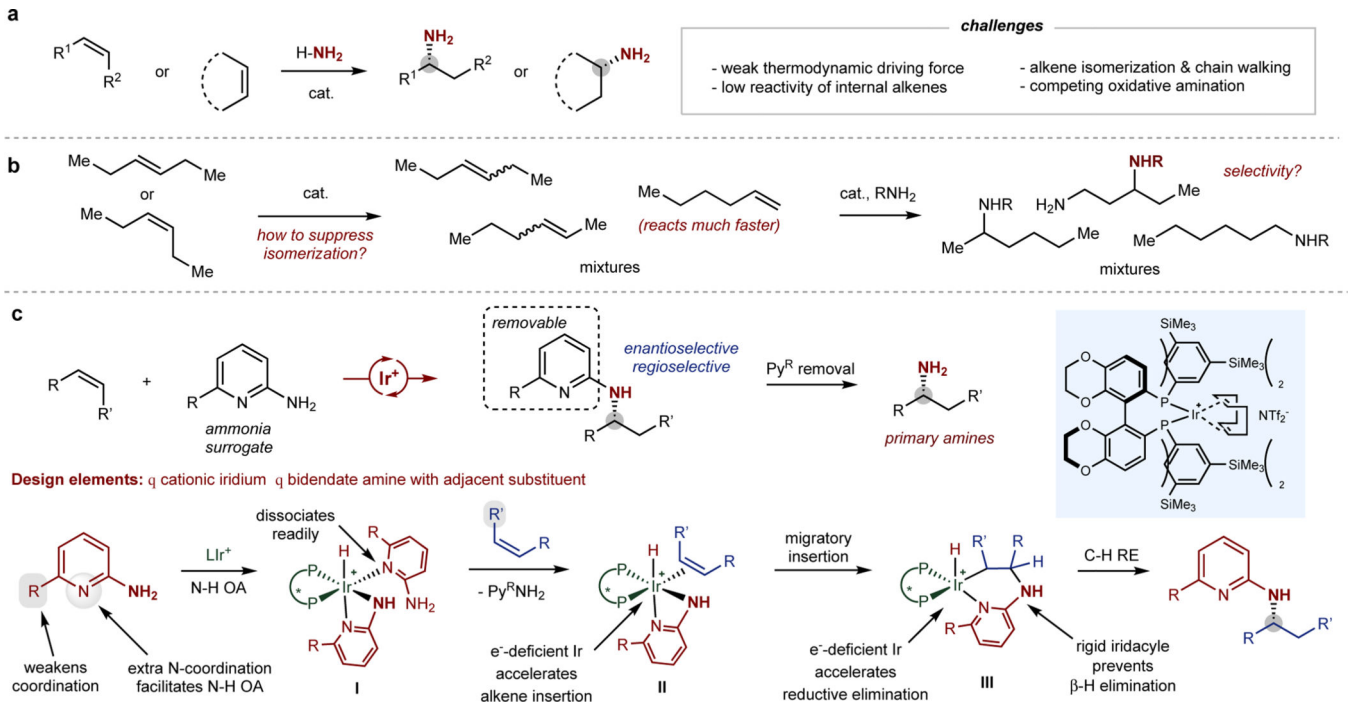

Fig. 1. Catalytic asymmetric hydroamination of unactivated internal alkenes.

a, Long-standing challenges and previous strategies for catalytic hydroamination of unactivated internal alkenes. **b,** Alkene isomerization that leads to a mixture of constitutional isomeric products. **c,** Design of a cationic iridium catalyst and an ammonia surrogate based on 2-aminopyridine to achieve asymmetric hydroamination of internal alkenes. OA, oxidative addition. RE, reductive elimination.

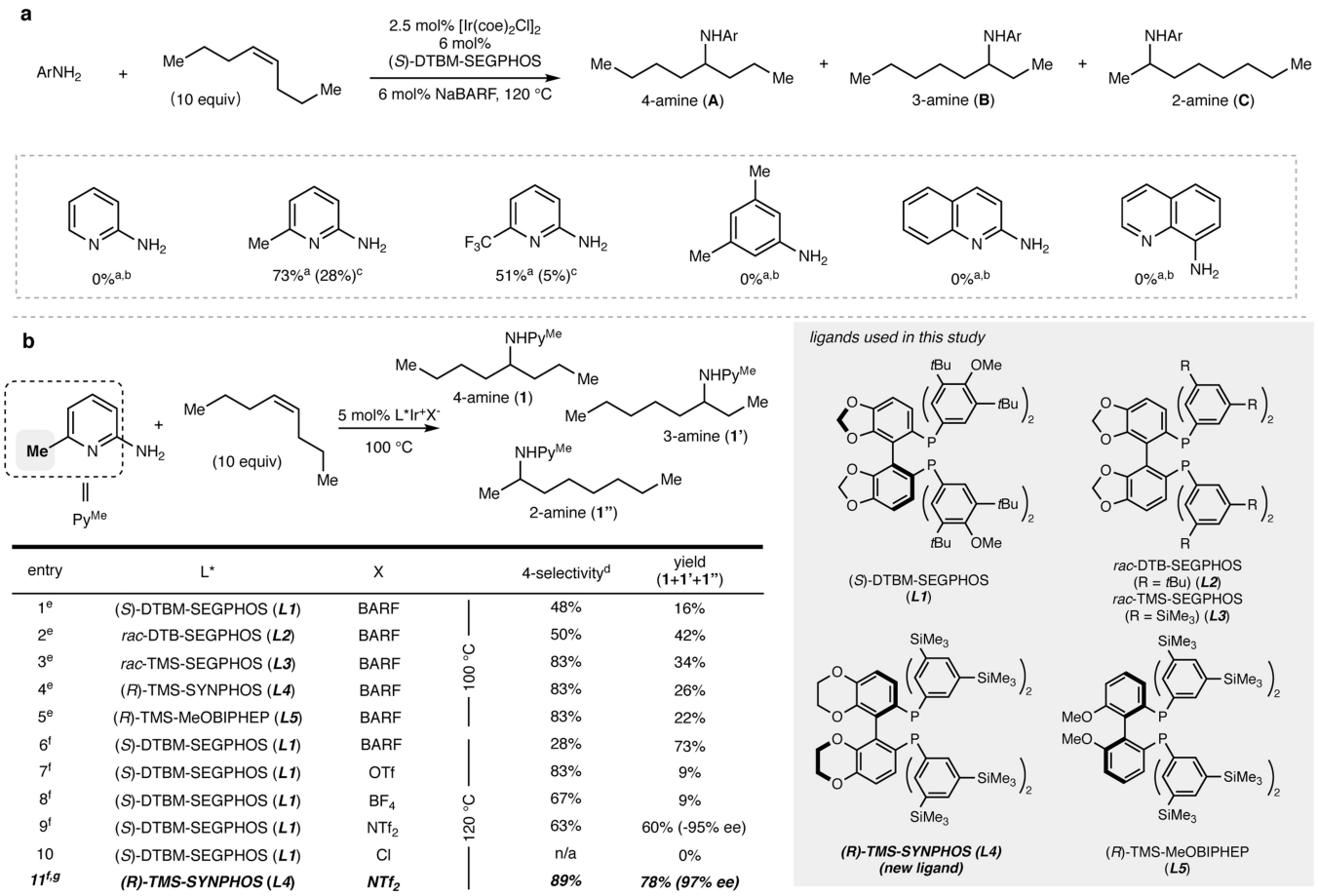

entry	L*	X		4-selectivity[d]	yield (1+1'+1")
1[e]	(*S*)-DTBM-SEGPHOS (***L1***)	BARF	100 °C	48%	16%
2[e]	*rac*-DTB-SEGPHOS (***L2***)	BARF		50%	42%
3[e]	*rac*-TMS-SEGPHOS (***L3***)	BARF		83%	34%
4[e]	(*R*)-TMS-SYNPHOS (***L4***)	BARF		83%	26%
5[e]	(*R*)-TMS-MeOBIPHEP (***L5***)	BARF		83%	22%
6[f]	(*S*)-DTBM-SEGPHOS (***L1***)	BARF	120 °C	28%	73%
7[f]	(*S*)-DTBM-SEGPHOS (***L1***)	OTf		83%	9%
8[f]	(*S*)-DTBM-SEGPHOS (***L1***)	BF_4		67%	9%
9[f]	(*S*)-DTBM-SEGPHOS (***L1***)	NTf_2		63%	60% (-95% ee)
10	(*S*)-DTBM-SEGPHOS (***L1***)	Cl		n/a	0%
11[f,g]	***(R)-TMS-SYNPHOS (L4)***	***NTf_2***		***89%***	***78% (97% ee)***

Fig. 2. Development of asymmetric hydroamination of unactivated internal alkenes with 2-amino-6-methylpyridine as an ammonia surrogate.

a, Identification of suitable ammonia surrogates to enable hydroamination of unactivated internal alkenes. **b,** Identification of reaction conditions to achieve asymmetric hydroamination and to suppress alkene isomerization. [a]Combined yield. [b]No reaction. [c]Defined as **A**/(**A**+**B**+**C**). [d]4-Selectivity defined as **1**/(**1**+**1'**+**1"**). [e]Conditions: 2.5 mol% $[Ir(coe)_2Cl]_2$, ligand, NaBARF, toluene, 100 °C. [f]Conditions: 5 mol% [L*Ir(COD)]X, toluene, 120 °C. [g]in 2-MeTHF.

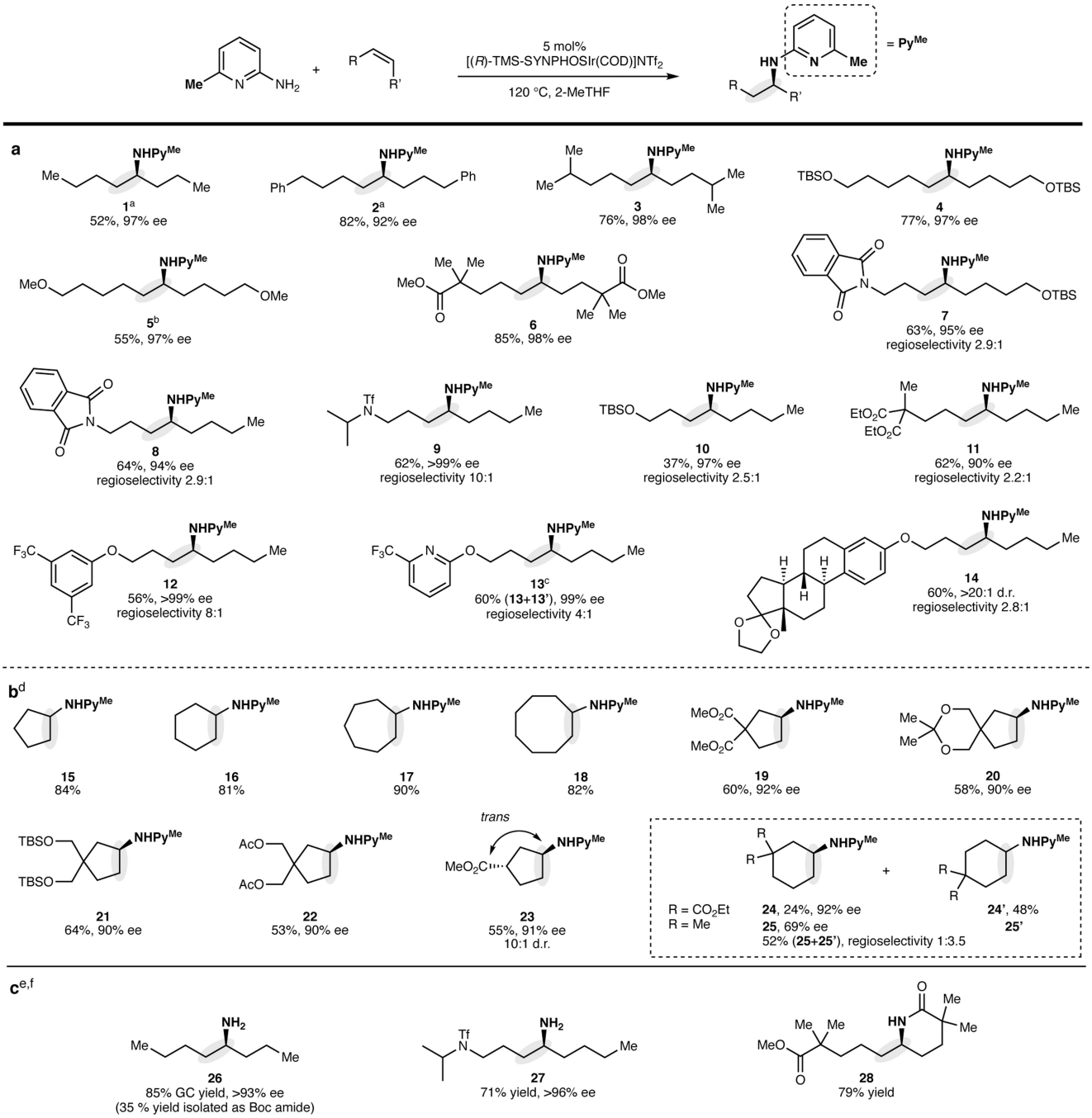

Fig. 3. Scope of internal alkenes that undergo the hydroamination.

a, Scope of asymmetric hydroamination of acyclic internal alkenes. **b,** Scope of hydroamination of simple cycloalkenes and of asymmetric hydroamination of substituted cyclic alkenes. **c,** Products from removal of the 2-(6-methyl)pyridyl group. [a]2.5 mol% catalyst. [b]7.5 mol% catalyst. [c]20 mol% catalyst. [d]Conditions: 2.5 mol% $[Ir(coe)_2Cl]_2$, 7.5 mol% (*S*)-DTBM-SEGPHOS, 6 mol% NaBARF, 1,4-dioxane, 120 °C. [e]Conditions: PtO_2, HCl, H_2 (1 atm); $NaBH_4$, THF/EtOH. [f]Enantioselectivities were determined after conversion

to the original hydroamination product by palladium-catalyzed cross coupling of the primary amine with 2-bromo-6-methylpyridine.

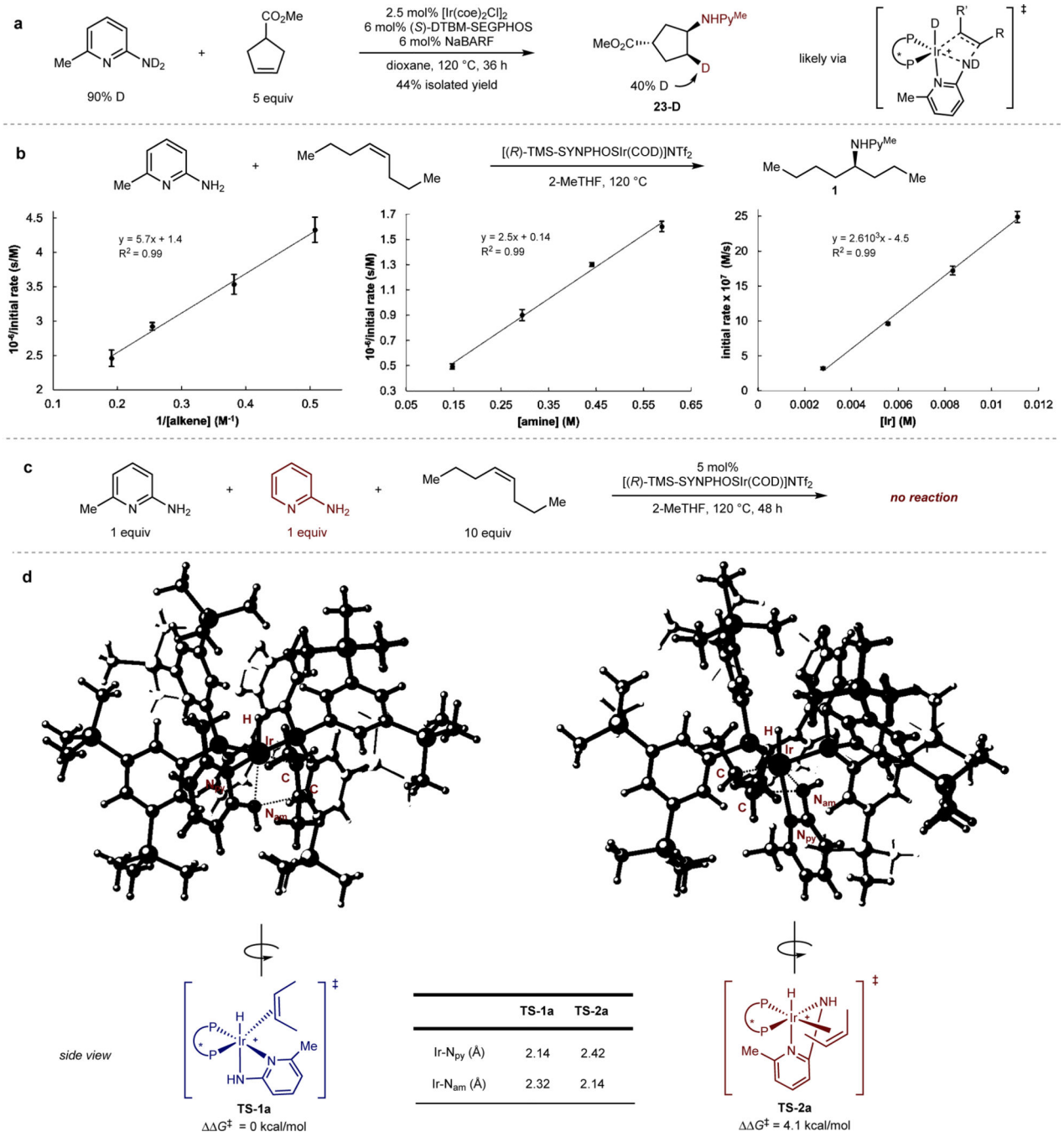

Fig. 4. Mechanistic study of the hydroamination.

a, Deuterium-labeling experiments. **b,** Experiments to reveal kinetic orders of each reaction component. **c,** Competition experiments using 2-amino-6-methylpyridine and 2-aminopyridine. **d,** Transition-state structures of alkene migratory insertion computed by DFT. Single-point energies were computed at the M06/6–311+G(d,p)/SDD/SMD(1,4-dioxane) level of theory with structures optimized at the B3LYP/6–31G(d)/SDD level. The ligand used for the calculations is (*S*)-TMS-SEGPHOS. The hydride is located trans to the amido ligand in the lowest-energy transition state (**TS-1a**) that leads to the (*R*)-enantiomer

but is located trans to the pyridyl group in the lowest-energy transition state (**TS-2a**) that leads to the (*S*)-enantiomer.